Polarization Study of Gamma Ray Bursts

THESIS

Submitted in partial fulfillment

of the requirements for the Master's degree

by

Tarun Jhangyani

Under the guidance of

Dr. Sunder Sahayanathan

Scientific Officer - F, BARC

Department of Physics

St. Xavier's College (Autonomous), Mumbai

2023

THESIS SUBMITTED

TO **ST. XAVIER'S COLLEGE, MUMBAI**

FOR THE **MASTER'S** DEGREE

IN **PHYSICS**

Name of the student: **Tarun Manohar Jhangyani**
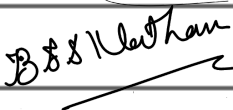
UID no.: **219112**

Name of the guide: **Dr. Sunder Sahayanathan**

Designation and affiliation of

guide: **Scientific Officer - F, BARC**

Dissertation title: **Polarization Study of Gamma Ray Bursts**

Submission date: **20/03/2020**

Signature of student**:**

Signature of guide:

ACCEPTANCE OF SUBMISSION

Name of the assigned

departmental mentor: **Dr. Manojendu Choudhury**

Designation of mentor: **Assistant Professor, St. Xavier's College, Mumbai**

Signature of mentor

(with date):

CERTIFICATION OF SUCCESSFUL COMPLETION OF THESIS AND VIVA

Signature of certifying authority: _____ Date: _____

Name and designation of certifying authority:

UNDERTAKING BY THE STUDENT

I declare that the work embodied in the thesis entitled **Polarization Study of Gamma Ray Bursts** represents my own contribution to the research carried out under the guidance of **Dr. Sunder Sahayanathan, Scientific Officer - F** from **Bhabha Atomic Research Centre.**

The work presented in this thesis has not been submitted for the award of any other degree to this or any other institute. References to other research studies have been duly acknowledged and included in the bibliography.

The thesis has been checked for plagiarism using the software Turnitin, and the soft copy of the report is being submitted along with this thesis.

20/03/2023

Date

Tarun Jhangyani

Name and signature of student

CERTIFICATE FROM GUIDE

I certify that the thesis entitled **Polarization Study of Gamma Ray Bursts** submitted by **Tarun Manohar Jhangyani** for the award of Master's degree, embodies original work done by him/her under my guidance.

This work has not been submitted to this or any other institute for the award of any other degree.

19/03/2023
Date

Dr. Sunder Sahayanathan
Scientific Officer - F, BARC
Name and signature of guide
Designation and affiliation

ACKNOWLEDGEMENTS

ABSTRACT

The shortest, most intense, and brightest explosions in the cosmos are called gamma ray bursts (GRBs). The two phases of Gamma Ray Burst (GRB) emission are the prompt and the afterglow. For the afterglow phase of GRBs, the origin and underlying process have been understood, although this cannot be true for the prompt emission phase. The quick emission has been attempted to be explained by a number of hypotheses, including the synchrotron mechanism and inverse Compton scattering. In order to distinguish between these emission mechanisms based on their unique polarization fingerprints, the measurement of hard X-ray and gamma-ray polarization is thought to be of great importance in the study of GRB prompt emission.

Due in large part to the challenging nature of measuring polarization in these bands, the hard X-ray polarization measurements of GRB prompt emission have not yet meaningfully limited the GRB theories. The goal of this particular thesis is to search for strong polarization signals in GRBs in order to comprehend the physics underlying the process. It has been experimentally confirmed that the AstroSat's CZT Imager (CZTI) is capable of performing polarization measurements in the energy range of 100 to 300 keV. This thesis examines the polarization of two GRBs using data from the AstroSat satellite's CZTI detector.

Modulation curve fitting and MCMC simulations are used to determine the polarization amplitude and polarization angle, and polarization status of GRB sources is confirmed if the Bayes factor $\frac{P(M_{pol}|D)}{P(M_{umpol}|D)}$ is more than 2. In this thesis, the polarization state of two GRBs is reported. Among the two, it is determined that GRB180427A is polarized, but GRB190928A is unpolarized.

Keywords:
Gamma Ray Burst, Prompt Emission, Polarization, CZTI, Astrosat, MCMC

TABLE OF CONTENTS

LIST OF TABLES

LIST OF FIGURES

ABBREVIATIONS

GRB   Gamma Ray Burst

BATSE   Burst And Transient Source Experiment

CRGO   Compton Gamma Ray Observatory

HETE-2   High Energy Transient Explorer 2

FRED   Fast Rise and Exponential Decay

CZTI   Cadmium Zinc Telluride Imager

IDL   Interactive Data Language

MCMC   Markov Chain Monte Carlo

PA   Polarization Angle

PF   Polarization Fraction

CHAPTER 1
INTRODUCTION TO GAMMA RAY BURSTS

1.1 What is a GRB?

Gamma-ray bursts (GRBs) are short bursts of gamma radiation. GRBs are dazzling and fleeting, lasting only a few seconds or so (sometimes hundreds of milliseconds). Due to their high luminosity during the course of their brief existence, they surpass all other gamma-ray sources. The convention for GRB naming is GRB YYMMDD, and it is dependent on the day that each GRB is found. If more than one explosion is discovered on a single day, the name is given a latin letter. GRB 991122A, for example, denotes the first GRB found on November 22, 1999.

1.2 Brief Historical Background

The United States' VELA military satellites, which were put into orbit to keep an eye on potential nuclear explosions both inside and outside the Earth's atmosphere, accidentally stumbled onto GRBs. Despite the fact that the first incidence was noticed in 1967, it took until 1973 for the scientific community to learn about cosmic gamma-ray bursts [9]. Several ideas were put forth shortly after the announcement in 1973 to account for the GRB's genesis. The number of bursts at the moment matched the number of models . The suggested sources included a wide range of astronomical objects, [7] including those at the solar system's outer limits and the extreme reaches of the observable cosmos. Similar to the theories that are thought to be responsible for the majority of galactic X-ray emissions, it was thought in the 1980s that close galactic neutron stars were the most likely candidates to explain GRBs [9].

Prior to the BATSE era, several missions examined GRBs and their characteristics and attempted to draw conclusions from the data that were significant. In addition to measuring the light curves of GRBs to look for potential periodicities, researchers also looked at their spectra to see whether they were thermal or non-thermal and to look for any potential spectral quirks. Contrary to the Galactic population theory, the distribution of GRBs appears to be isotropic, non-homogeneous [7], [9], and not focused on the Galactic Plane. The discovery of isotropy led to the conclusion that the sources were galactic yet close, with a distance scale lower than the scale height of the Galactic Disk [9], maintaining the idea that

they are galactic. This isotropy ran counter to the long-held belief that GRB sources are located both within and in the plane of the galaxy [9]. But for some, it was a big enough drawback to propose extragalactic and cosmic hypotheses.

1.3 Key GRB missions, Discovery and Breakthroughs

The Burst And Transient Source Experiment (BATSE), a project of the Compton Gamma Ray Observatory (CRGO), was initiated by NASA in 1991 [7], [9]. The duration, rapid variation, absence of periodicities, and sentences of two separate GRB types—short and long—were confirmed. They confirmed and in-depth examined the energy spectra's non-thermal nature [9] and the spectrum's variation during a burst. Soon after BATSE, the isotropy of the angular distribution, which had previously been seen, was verified for hundreds of coarsely localized GRBs. The most noteworthy outcome of BATSE is the combination of the unquestionable isotropy and non-homogeneous distribution of the GRB dispersion in the sky [9].
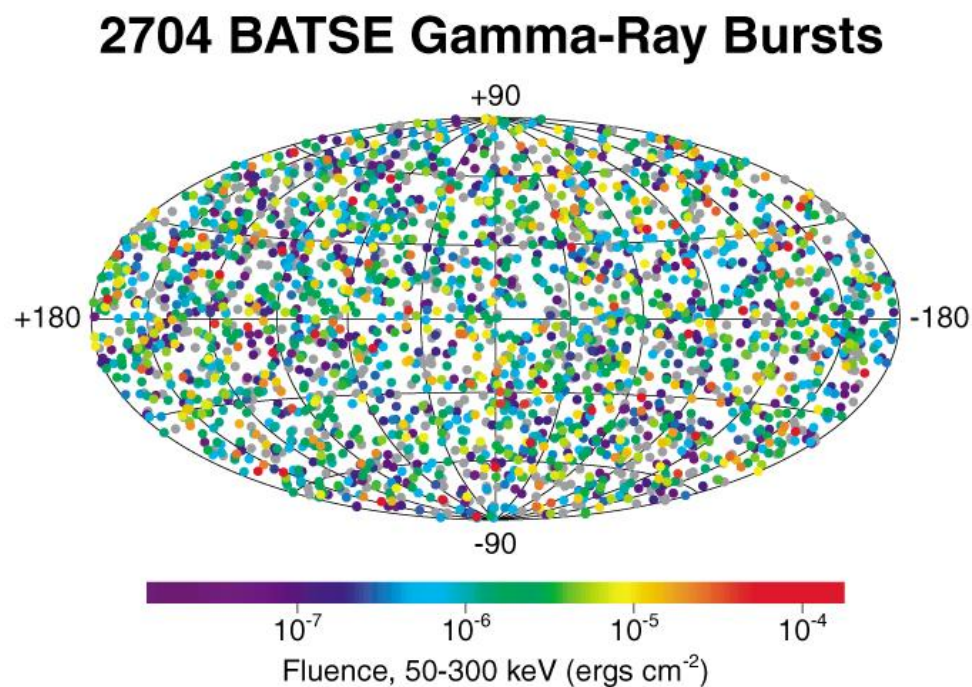

Figure 1.1: Distribution of GRB sources in the sky. The chart depicts the locations of approximately 2700 GRBs found by the BATSE. Credit: https://heasarc.gsfc.nasa.gov/docs/cgro/batse/

The BATSE data provided strong evidence against a GRB origin connected to local neutron stars in the Galactic Disk, and even the expanded Galactic Halo models had difficulty

explaining them [9]. This made the idea that the GRBs might be far from Earth more widely accepted. Despite the amazing results of BATSE, the lack of counterparts at all wavelengths prevented the identification of GRB origins. How far away are GRBs? was the question that was asked the most. What precisely are they? How are gamma rays produced?

The location of GRB sources might be pinpointed with great accuracy after BATSE. The Italian-Dutch BeppoSAX mission was successful in its search for the counterpart [7], [9]. It was a noteworthy development because, for the first time, quick GRB localizations were accurate enough to allow for the observation of GRB afterglow at optical and radio wavelengths. We determined the host galaxies and distances of the recently discovered GRBs counterparts. For instance, one burst was discovered at a high redshift of z = 3.42. The host galaxy, a star-forming galaxy, produced a GRB when the universe was only 2 billion years old [9]. With only a few additional insights, the missions that came after BeppoSAX, such as HETE-2 and Swift, solved the problems concerning the speed of localization of sources..

1.4 Characteristics and properties of GRBs

1.4.1 Types of GRBs based on Light curve and Timescales

Gamma rays with an energy range of a few hundred keV to GeV are detected as part of the GRB's prompt emission. Several milliseconds to many hundreds of milliseconds are the range of duration for GRBs. None of the other cosmic objects have only this one special attribute. Their light curves also exhibit a wide range of shapes [7], rising swiftly and declining slowly or being reasonably symmetric, with one or several spikes emerging in quick succession or with large intervals in between. Most of the time, they differ by milliseconds.

Fast Rise and Exponential Decay (FRED) [9] was the name of one of the several classes. Two subclasses of bursts in terms of duration and spectrum have been identified by the aggregate of a sizable sample of observed GRBs. Short bursts are defined as those that last under two seconds, while lengthy bursts are defined as those that continue longer than two seconds [7], [9]. A little burst normally lasts 0.5 seconds, but a huge burst lasts 30 seconds. The statistical classification of long and short bursts have been studied, with two significant peaks centering about 0.3 seconds and 20 seconds, respectively, and a low at

roughly 2 seconds [9], BATSE effectively demonstrated the bimodality of GRB durations.
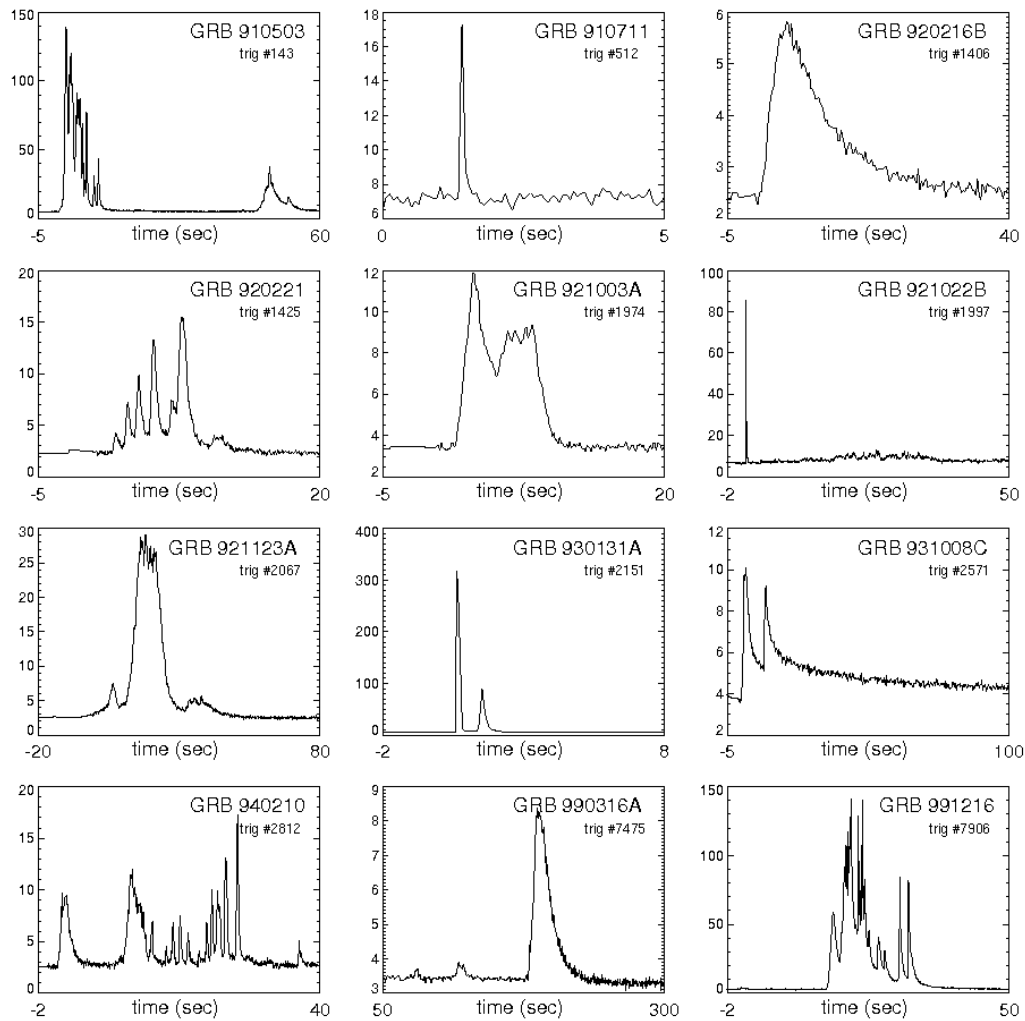
Figure 1.2: A collection of light curves (the counts of gamma-ray photons observed as a function of time) of various GRBs' prompt emission. Credit: https://www.wikiwand.com/en/File:GRB_BATSE_12lightcurves.png
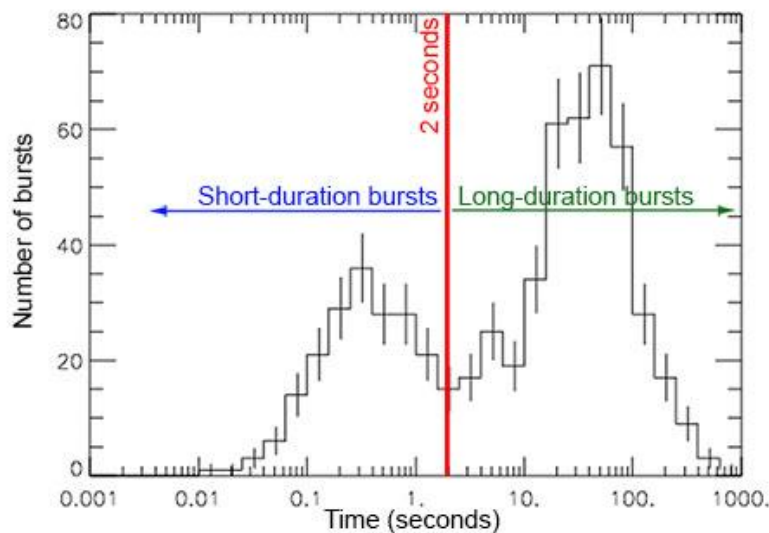
Figure 1.3: Bimodal distribution histogram plot. Based on the bimodal time distribution, GRBs are classified into two types. Credit: https://imagine.gsfc.nasa.gov/educators/gammaraybursts/starchild/page2.html

1.4.2 Classification based on Spectra

GRBs can be categorized based on spectrum characteristics in the same way that accumulation of sizable samples of GRBs classifies them based on time scales. The majority of the energy of GRBs, between hundreds of keV and a few MeV [9]. Their spectra, which span a wide range of frequencies and energies, are shaped like a broken power law or an exponential function followed by a power law [9]. The distribution switches from one power law function to another at a characteristic peak that corresponds to the highest energy (Epeak or Ep) [7], [9].
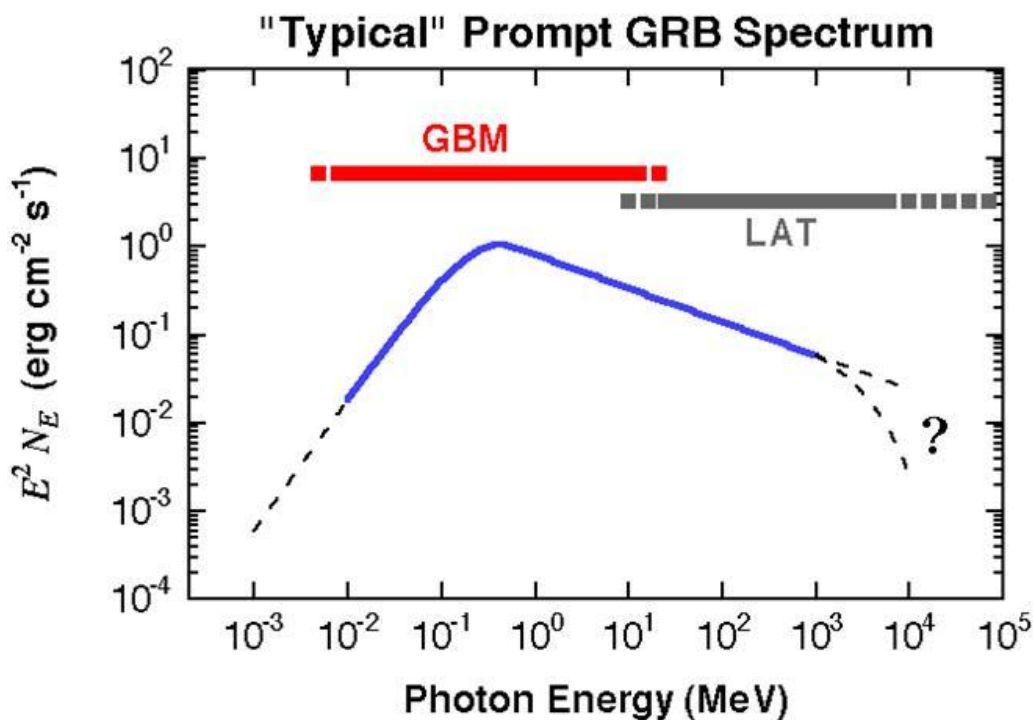
Figure 1.4: Typical spectra of the prompt phase of GRB. Credit: Understanding GRBs | Multiwavelength Astronomy (uchicago.edu)

The proportion of fluence measured in a high-energy channel compared to a low-energy channel is the definition of the hardness ratio, a detector-based gauge of spectral shape [7]. Depending on the instrument, these channels could be different [7], [9]. The

statistical study of GRBs based on hardness ratio shows that Contrary to longer bursts, shorter bursts frequently have harsher spectra.
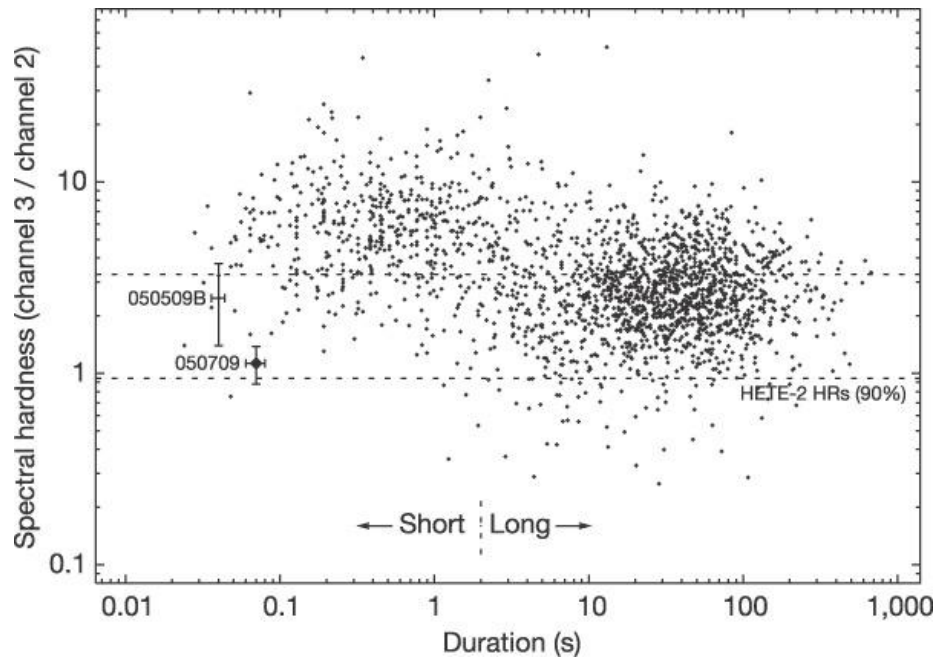
Figure 1.5: Distribution of the hardness ratio in relation to T_{90}. T_{90} is the period of time when photon counts rise by 95 percent above background. Credit: https://www.researchgate.net/figure/The-classic-BATSE-duration-spectral-hardness-diagram1 GRB-050709-large-filled-diamond_fig2_7557890

1.4.3 Different Phases of GRB

Gamma rays are produced by the prompt emission phase of GRBs, which is followed by the afterglow phase (generally extending from X-rays to Radio waves). The huge improvement in source sky position accuracy [7], [9] made possible by afterglow detections is what gives them their significance. Finding counterparts allows one to estimate the host galaxy's redshift, which gives insight on the source's luminosity and overall energy production as well as possible geometry [9]. The afterglow is stable, in contrast to the chaotic prompt emission [9].

CHAPTER 2
THEORETICAL MODEL AND POLARIZATION

2.1 The Standard Fireball Model

GRBs are produced at cosmological distances; assuming isotropic energy emission, the computation of their radiated energies from the recorded fluence yields an enormous amount of energy production of $\sim 10^{54} ergs$ [9]. The millisecond variability of GRBs limits their size, and when combined with their enormous energy production in the absence of special relativistic effects, it suggests that the source is compact because so much energy (more energy than the sun emits during its lifetime) is produced in such a small volume [9]. The massive quantity of energy contained within a tiny space suggests an electron, positron, and gamma photon soup. This is the foundation for the fireball model, which debuted in early 1978 [9].

The origins of GRB creation should be compact despite the fact that such enormous energies have been seen in other occurrences like supernovae [9]. Yet, gamma rays shouldn't be released from a compact source with such a high brightness! When high-energy photons collide, electron-positron couples can result. While significant flux is observed above 1 MeV to multiple 10 GeV, the source cannot emit non-thermal radiation due to the huge optical depth value [9], which suppresses photons over 1 MeV. Compactness is the problem. In contrast to the well-established fact that GRBs are located at cosmic rather than galactic distances, this type of fireball model stated that the enormous flux over 1MeV could only be created by close sources. Relativistic expansion solves the compactness problem [7], [9]. The answer is that the fireballs must initially be opaque [7], [9] in order to create pairs. The fireballs are predicted to grow relativistically because of this high degree of opacity (because luminosity of source is many orders of magnitude higher than the Eddington luminosity [7]). A fireball's extremely relativistic expansion changes its radiation by shortening perceived timeframes and blueshifting observed photons (In the observer frame, an X-ray photon changes from an X-ray to a gamma ray [9]).

Thus, relativistic expansion offers a highly effective way to lower the rate of pair creation: in the moving source frame, photons are softer by a factor $\mathbf{\Gamma}$ (the Lorentz factor of

the relativistic flow), and they originate from a region with a typical size of $\Gamma^2 c\Delta t$ [7], [9] (rather than ct for a stationary source), which lowers their density significantly. Moreover, relativistic beaming allows only a tiny portion of the source to be seen, which lowers the amount of pairs that are produced. Optically measured depth (τ) for relativistic motion is highly dependent on (Γ) [7], [9]. The optical depth must normally be very shallow, $\tau < 1$, for a typical GRB, in order for high-energy gamma photons to escape. This results in a Lorentz gamma factor $\Gamma \geq 100$ [7], [9].

Gamma-ray bursts were equally difficult to explain in terms of the relativistically expanding fireball. Rather than having non-thermal spectra, the radiation that was released had quasi-thermal spectra [9]. The fireball shock model, which postulates that afterglow radiation is produced by the shock of the fireball [9] on the external surrounding medium, was put forth as a potential remedy. The internal shocks have the best understanding of the light curves of the prompt phase [9]. These models are based on the hypothesis that shocks caused by ultra-relativistic outflows are likely to result in the internal kinetic energy of the fireball being converted back into internal energy of non-thermal electrons and radiation [9]. The medium contains a large number of electrons, which accelerates them into shocks and raises their energy. To form the GRB spectra that may be viewed, these particles will eventually radiate through inverse Compton scattering, synchrotron emission, or maybe both and etc. To understand the emission mechanism such as Synchrotron, Inverse Compton Scattering, in depth refer to chapter 6 & 7 of reference 8 and chapter 5 of reference 9.
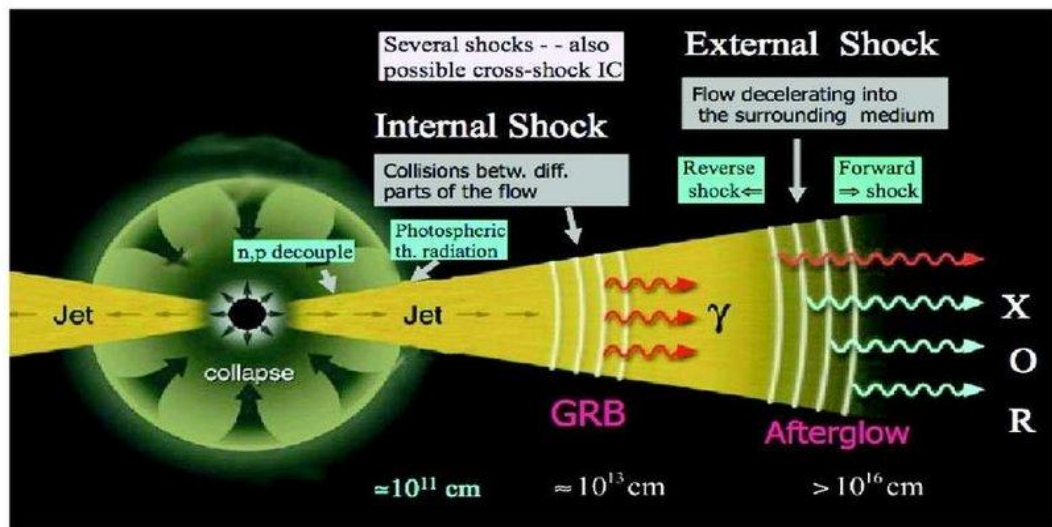

Figure 2.1:   A schematic diagram of the fireball model for GRBs. Credit:

2.2 Need for Polarization Study

GRBs are thought to be closely related to the development of stellar-mass black holes in the middle of enormous star explosions or the collisions of compact stellar binaries [2], [3]. The first burst of high-energy emission, known as prompt emission, is believed to be created by a jet close to the black hole [3], while the long-lasting multi-wavelength afterglow emission is likely to be caused by the GRB jet's interaction with the atmospheric medium distant from the compact object. Despite a high number of GRBs being picked up by the sensitive detectors of the Swift and Fermi sensors, the prompt emission mechanism is still not well understood [1], [2], [3] because of the diversity, severe unpredictability, and short length of this phase.

Both the synchrotron mechanism and inverse Compton scattering are thought to have produced the rapid emission. Moreover, a few instances provide proof of a thermal blackbody component [2], [3]. In order to distinguish between these emission mechanisms based on their distinctive polarization fingerprints [3], the measurement of X-ray and gamma-ray polarization is thought to be of great help in the study of GRB prompt emission. Because it is challenging to determine polarization in these bands, the hard X-ray polarization of GRB prompt emission observations that are currently available have not greatly limited the GRB theories [3]. Particularly, a statistical analysis of the polarization of GRBs may offer important limits on the geometry and radiation mechanism at play. Several GRB model assumptions are expected to require the validation of X-ray and gamma-ray polarization data of the rapid emission of gamma-ray bursts (GRBs).
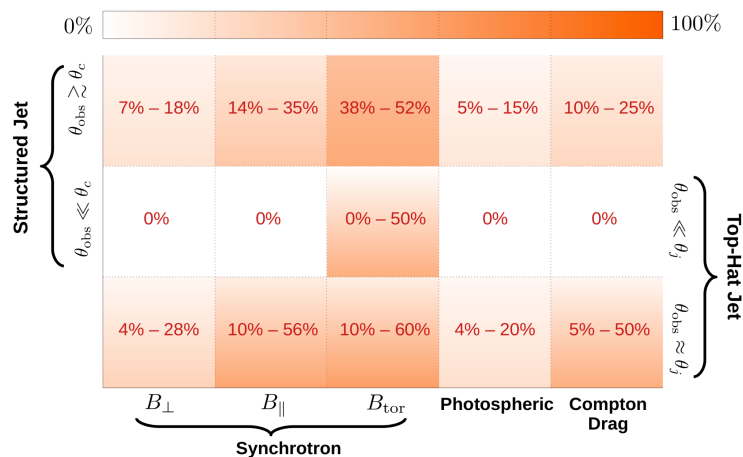

Figure 2.2: Polarization fraction expected for different radiation models (Compton drag model, Synchrotron ordered model, Synchrotron random model, and Photospheric model) and jet structures along with jet viewing angle geometry. Credit: Reference 5.

2.3 Polarization, Polarimetry and CZTI

2.3.1 Polarization

The polarization of photons reveals the fundamental electromagnetic wave nature of these particles. A photon is a separate bundle of magnetic and electric fields that are pointed in a direction opposite to the direction of motion [4]. Maxwell's equations state that the fields evolve across time and space. Polarization explains how the fields are organized. By definition, each photon is polarized. Yet, distinct photons from the same source could have various polarisations [4]. If the polarization angle spread is uniform, the source does not exhibit any net polarization [4]. In the event that it does not, the source is polarized overall. Non-zero net polarization necessitates a net divergence from spherical symmetry in the physical geometry of the astrophysical system or the magnetic field configuration [3], [4].

2.3.2 Polarimetry - How exactly polarization is measured?

In order to quantify polarization, it must first be converted into another observable variable, usually intensity or position [1], [2], [3], [4]. These instruments use a technique to count the number of photons produced in a given amount of time, calculate the energy of the radiation (by converting it to heat or charge), and determine the positions of the radiation, or more precisely, [4] the locations where the radiation interacts to deposit charge.

Have a look at a single spinning linear polarization analyser. The corresponding detector measures the number of photons at each angle of the analyzer as it rotates. The modulation curve is the histogram of counts as a function of rotation angle [4] that results.
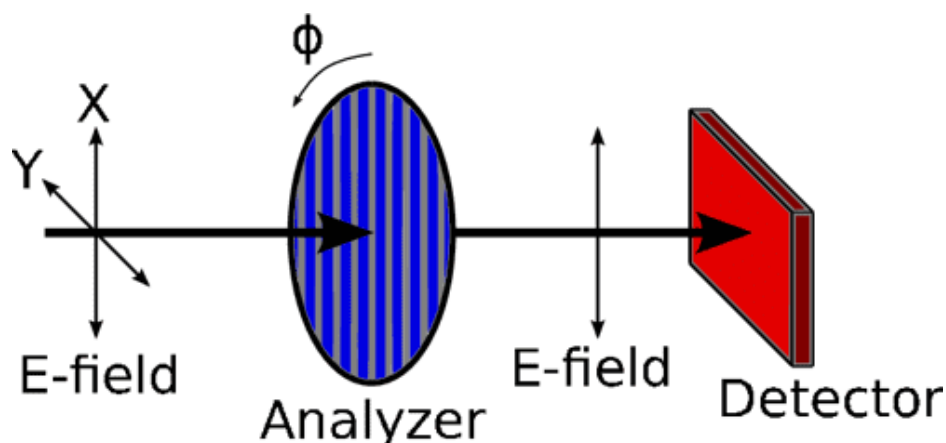
Figure 2.3: Schematic diagram of polarization measurement. Rotating a linear polarization analyzer causes the corresponding detector to record the number of photons (counts) at each angle as a modulation curve, as seen in Figure 2.4. Credit: Reference 4.
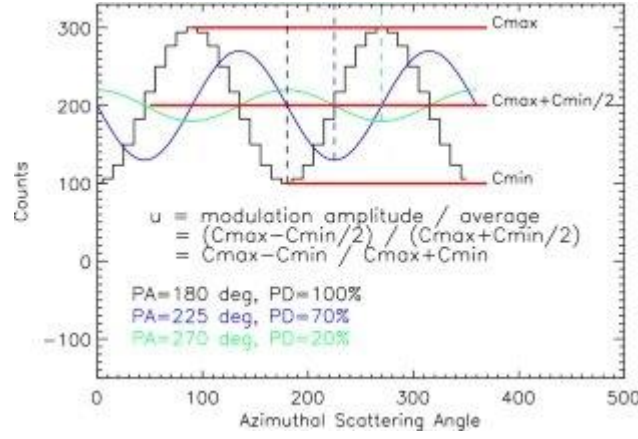
Figure 2.4: A diagram of a modulation graph. An illustration of a modulation signature for radiation that is highly, medium, and low polarized (black, blue, and green, respectively). Credit: Reference 1.

The general equation for the modulation curve can have the form:

$$C(\phi) = A + B\cos^2(\phi - \phi_0) \tag{2.1}$$

The other form is:

$$C(\phi) = A\cos(2(\phi - \phi_0 + \pi/2)) + B \tag{2.2}$$

A, B and ϕ_0 referred to as the fitting parameters.

ϕ_0 is called the polarization angle at which maximum intensity is recorded.

ϕ is the azimuthal angle in relation to a specific reference axis on the detector plane.

The standard procedure for calculating the modulation amplitude from the modulation curve for any unknown polarized radiation is to first normalize the modulation amplitude in comparison to the modulation amplitude for 100% polarized radiation. C_{max} and C_{min} are the maximum and minimum number of counts in the modulation curve (μ_{100}) [1]. μ_{100} is estimated from simulations.

The modulation amplitude is defined as:

$$\mu = \frac{C_{max} - C_{min}}{C_{max} + C_{min}} = \frac{A}{B} \tag{2.3}$$

The Polarization fraction is given as:

$$PF = \frac{\mu}{\mu_{100}} \tag{2.4}$$

18

CHAPTER 3
RESEARCH METHODOLOGY

3.1 The Framework of the Research

The two brightest GRBs, GRB 190928A and GRB 180427A, have each been the subject of a polarization analysis in this thesis. The AstroSat CZTI provided the information needed to analyze these two GRBs. A double event light curve is produced as part of the AstoSat CZTI's polarization pipeline. This separated information from the double event provides the azimuthal angle distribution for each GRB, which is utilized to calculate the characteristics unique to polarization. These parameters are additionally calculated using the MCMC approach. The Bayes Factor, which indicates whether the observed GRB has a polarization signature, is then determined using Bayesian statistics.

The operating system - Ubuntu, softwares - Heasoft, and IDL must be installed in order to do the analysis. The cosmic astronomy datasets for observations in the extreme electromagnetic wave bands, as well as for datasets for the cosmic microwave background (CMB), are stored in the HEASARC, which is NASA's authorized multi-mission astronomy archive. An interactive data language called IDL is used for data analysis. The Ubuntu (Linux) system serves as the sole platform for the Polarization study. The computer language used in this thesis to investigate polarization is called IDL. In addition to the IDL Language, supporting background software includes the HEASARC Heasoft programme. All the instructions required to complete the analysis are already present in the IDL Language.

3.2 GRB Polarimeter - CZTI

On September 28, 2015, India launched AstroSat, the nation's first specifically designed astronomical satellite, and it has since been successfully in operation. Using a number of CZT detectors, the AstroSat's Cadmium Zinc Telluride Imager (CZTI) instrument is a large-area spectroscopic sensor. CZTI is made up of a 64-detector array of CZT modules, each measuring 5 mm thick and offering excellent quantum efficiency and precise spectral resolution in a wide energy range between a few keV and a few hundred keV [1], [2], [3]. Each detector module is then further divided into 256 pixels, each of which has a nominal size of 2.5 mm by 2.5 mm [2], [3].

The device can image in the energy range of 20–150 keV thanks to a tantalum coded mask that is 0.5 mm thick. CZTI has a time resolution of 20 μs [2], [3]. CZTI also functions as a sensitive Compton polarimeter for strong X-ray sources at higher energy in addition to the spectroscopic and timing research. To understand Compton polarimetry in detail refer to reference 6. Compton scattering, which occurs most frequently perpendicular to the direction of the incident polarization, causes a sinusoidal modulation in the distribution of azimuthal scattering angles. The flying configuration has been shown to be capable of monitoring polarization during extensive experiments and modeling analyses carried out during CZTI's ground calibration [3]. Due to the increased transparency of the collimators and the transparency of the supporting structure in the energy range of 100-300 keV [2], [3], CZTI acts as an open detector and detects high-energy transient events like GRBs occurring all over the sky [3]. The selection criteria for the Compton events have been discussed in detail in reference 2 and 3.

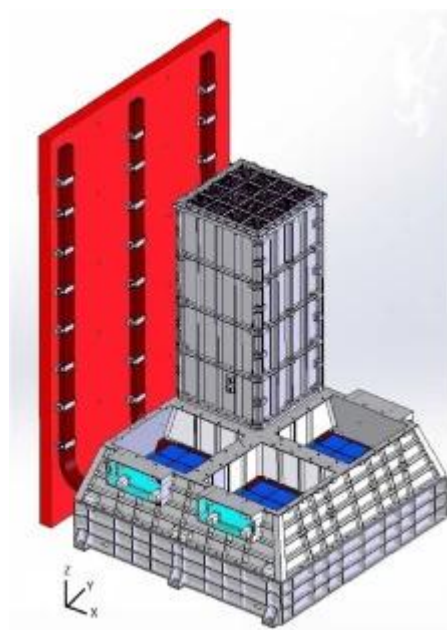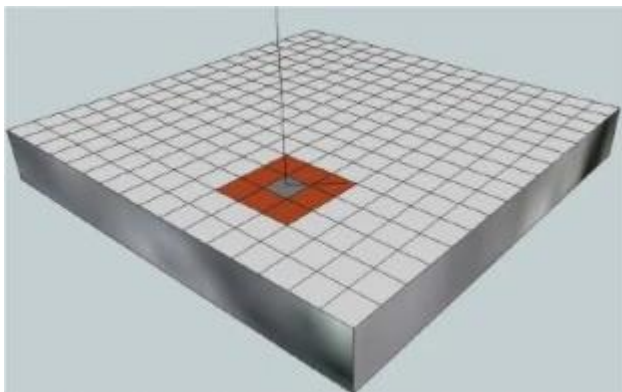Figure 3.1: A schematic diagram of CZTI onboard the AstroSat mission. Credit: Reference 1

Figure 3.2: Compton Polarimetry in CZT detectors. The azimuthal Compton scattering angle for polarization analysis is provided by the pixel with low-energy deposition shown in gray or the first event and one of the neighboring 8 pixels with high-energy deposition shown in red or the second event. Credit: Reference 1

3.3 How are Modulation amplitude and Polarization Angle estimated?

The polarization signature can only be derived once the azimuthal scattering angle distribution for GRB photons has been determined. For combined background and GRB events, an eight-bin azimuthal angle distribution is produced [1], [3]. After that, to get the source distribution, the total distribution is subtracted from the azimuthal angle distribution for background events alone [2], [3]. The background distribution is created by averaging [3] the azimuthal count distributions before and after the GRB. Two distinct methods—(A) standard fitting of the geometry adjusted modulation curve by a sinusoidal function and (B) using Markov chain Monte Carlo (MCMC) simulations - to obtain the posterior probability of parameters (A, B, ϕ_0) and eventually calculating the bayes factor to validate polarization percentage.

  A) *Fitting of Modulation curve*

  In this method, the polarization angle and modulation amplitude are calculated by fitting a cosine function to the modulation curve [1], [3]. This is done using previously existing fitting algorithms in IDL. The necessary parameters are provided by the fitted cosine curve, such as the modulation amplitude, which is used to calculate the polarization percentage and polarization angle. (Refer section 2.3.2)

  B) *Using MCMC simulations*

  An MCMC technique is used in this instance to estimate the modulation amplitude, the polarization angle, and associated uncertainty [3]. The simplicity of the fitting process and the robustness of the parameter uncertainty estimation when compared to fitting of the modulation curve are the reasons for adopting the Bayesian statistics technique. The modulation amplitude, polarization angle, and particularly their uncertainties [2], [3] are therefore estimated using the MCMC technique. MCMC simulations for a high number of cycles (around a million) are run. The likelihood is calculated for each iteration using arbitrarily selected parameter values from the model. (Equation 2.1 or 2.2). The posterior likelihood for a given iteration is contrasted with that of the preceding iteration to determine whether a set of parameter values for a given iteration should be accepted or rejected [2], [3]. In order to accept the parameter values, the posterior probabilities ratio must be bigger than unity. The

parameter values are then approved or rejected by comparison of the posterior odds for iterations with a ratio less than unity [3]. This method computes the posterior likelihood for these iterations starting from a homogeneous distribution of parameter values (A, B, ϕ_0) [2], [3].

Both of the aforementioned techniques for determining modulation amplitude and polarization angle are carried out automatically by means of IDL instructions.

3.4 Confirmation for Polarization - Calculation of Bayes Factor

Despite the strong modulations seen for the GRBs, further research is necessary before making any claims about the detection of polarization. replicating changes like these in the distribution of azimuthal angles. This is significant because, for the majority of GRBs, the modulation amplitude is a positively definite [3] amount and photons registered are very few. To calculate this chance probability, the use of Bayesian statistics has been applied. This is done by computing the Bayes factor for the constant model (for unpolarized photons) and the sinusoidal model (for polarized photons), where the Bayes factor is defined as the ratio of the marginal likelihoods of the models: $B_{21} = \frac{P(M_{pol} \mid D)}{P(M_{umpol} \mid D)}$ assuming equal prior probabilities for the models (*M1* and *M2*) [3]. The posterior probability is integrated across the parameter space to get the likelihood function, or *(P(M | D)) [3]*.

While the value of the Bayes factor, B_{21}, required to unequivocally favor the polarized model over unpolarized radiation that mimics the polarization signature is subject to interpretation, in this study a Bayes factor of > 2 [3] is used as the threshold for polarization measurements confirmation.

3.5 Polarization Analysis - Procedure

The steps are as follows:

Step A: Install the Ubuntu Operating System in Dual Boot Mode

Step B: Install the HEASARC Heasoft software using Command Prompt in Ubuntu

Step C: Install the IDL Programming Language using the Command Prompt

Step D: Setting up the codes and GRB data files (provided by the guide)

Comprehensively,

1. There are List of codes and supporting files needed for analysis already provided and all these required codes and files are kept inside a folder called "GRB_Polarization_Analysis"

2. Inside "GRB_Polarization_Analysis", GRB folders for each particular GRB are created and data files specific to the GRB are created.

3. Enter the "GRB_Polarization_Analysis" folder from the command prompt

4. Initialize the Heasoft Software using the "heainit" command in the command prompt.

5. Initialize the IDL language using the "idl" in the command prompt

Step E: Polarization Analysis Steps:

1. To obtain the single and double event light curve and select the region of prompt from the light curve for Polarization analysis.
   - Compile and run:
     .com comp_event_extract_t90_ver2
     comp_event_extract_t90_ver2,'./GRBYYMMDD/'
   - Light Curve is plotted, Use the cursor to select the zoom version of the burst region. Click well before and after the GRB so that pre and post-GRB background can be seen. Select around 500 seconds before and after burst region such that ample duration of background is present for selection in analysis
   - Pre-Background Duration Selection:
     Two windows pop up successively. The IDL terminal asks to choose the pre-background start and stop time sequentially using the cursor. Choose a stable background around 300 sec. Avoid the background too close to the burst's start time, keeping a difference in background stop time and burst's start time around 50 secs.
   - GRB Duration Selection:
     The terminal asks for "Burst Start Time (in AstroSat Seconds example: 219745960.0d0):", write it in "*********.****.d0" where d0 is for precision. The burst's start time is UTC+t1, enter from the table
   - Post-Background Duration Selection:

Two windows pop up successively. The IDL terminal asks to choose the pre-background start and stop time sequentially using the cursor. Choose a stable background around 300 sec. Avoid the background too close to the burst's start time, keeping a difference in background stop time and burst's start time around 50 secs.

- Output Files: single event and double event light curve, single event and double event files based on polarization selection criteria are stored automatically in the respective GRB folder.

2. Fitting of the modulation curve over the selected region of compton events
   - Compile and run:

     .com azimuthal_dist_ver4

     azimuthal_dist_ver4, Energy_start, Energy_end,'./GRBYYMMDD/',/mass

     (Energy_start (typical) = 100 (<Energy_end)

      Energy_end (typical) = 600 (<800))
   - Output Files: , azimuthal distribution plots, azimuthal distribution files are stored automatically in the respective GRB folder.

3. Run MCMC
   - Compile and run:

     .com call_mcmc_ver1

     call_mcmc_ver1, './GRBYYMMDD/', /bayes_therm, 'Energy_start',' **Energy_end',background',/int_plot**

     (Energy_start (typical) = 100 (<Energy_end)

     Energy_end (typical) = 600 (<800)

     background : 'pre'/'post'/'prepost')
   - Output: contour plot, modulation curve after mcmc fit, polarization parameter data file, fitted parameter plots are stored automatically in the respective GRB folder.

Each of the above mentioned steps are carried out for both the GRBs GRB 180427A and GRB 190928A. The data required to carry out analysis is given in table 1.

Name of the GRB (Detectors)	RA (deg, J2000)	DEC (deg, J2000)	Localization (degrees)	UTC	Burst Interval (s)	(t_1, t_2) (s)	Incident Direction (θ, ϕ) (degrees)
GRB 180427A (GBM)	283.33	70.3	1.0	262521423.0	13.01	(0.15, 13.16)	40.81, 257.79
GRB 190928A (Konus - Wind)	36.57	29.46	2.1	307372337.0	119.97	(-2.70, 117.26)	57.69, 231.26

Table 1: Information from GRBs chosen for CZTI's Polarization investigation.

UTC - Coordinated Universal Time

t_1 and t_2 are trigger start and end time

RA - Right Ascension

DEC - Declination

CHAPTER 4

RESULTS AND DISCUSSIONS

4.1 Results

This study presents the results of a detailed investigation of the GRBs found by CZTI aboard the AstroSat spacecraft, as well as the hard X-ray polarization measurements for two GRBs.
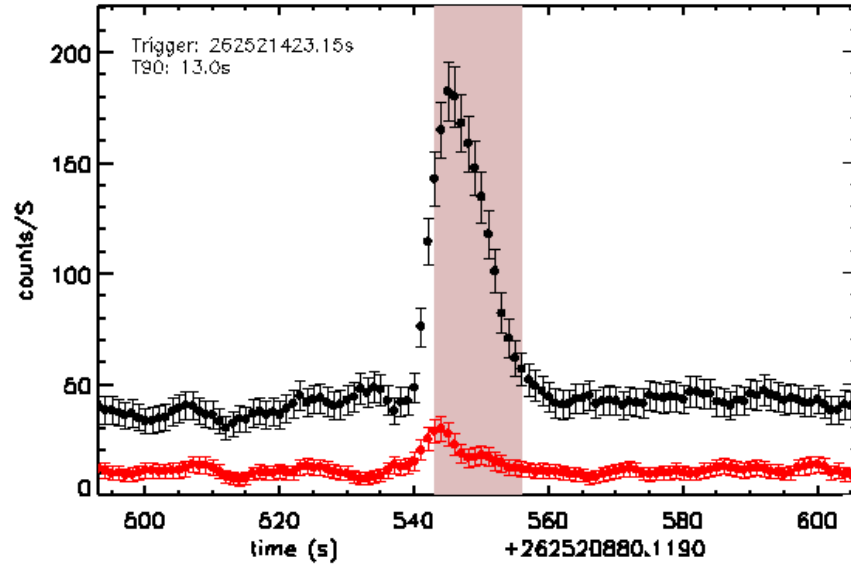
4.1.1 GRB 180427A

Figure 4.1: The GRB 180427A light curve. For polarization research, the light curve's shaded prompt emission phase is employed.
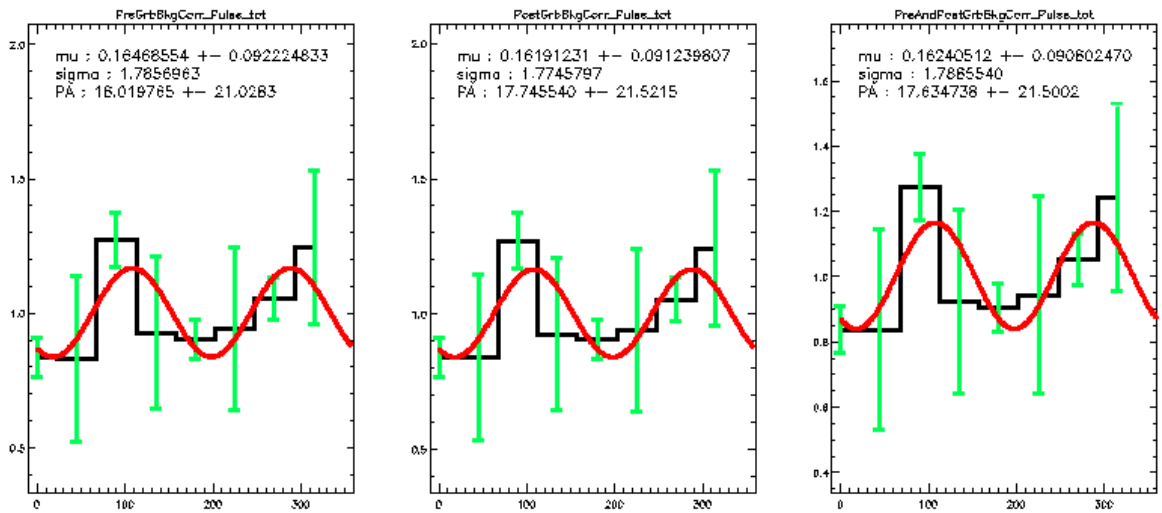
Figure 4.2: Fitted Modulation curve for GRB 180427A. The pre-GRB background radiation's adjusted modulation curve is shown on the graph to the left. The corrected modulation curve for the background radiation from post-GRB is shown in the middle of the graph. The corrected modulation curve for the background radiation before and after a GRB is shown in the graph to the right.
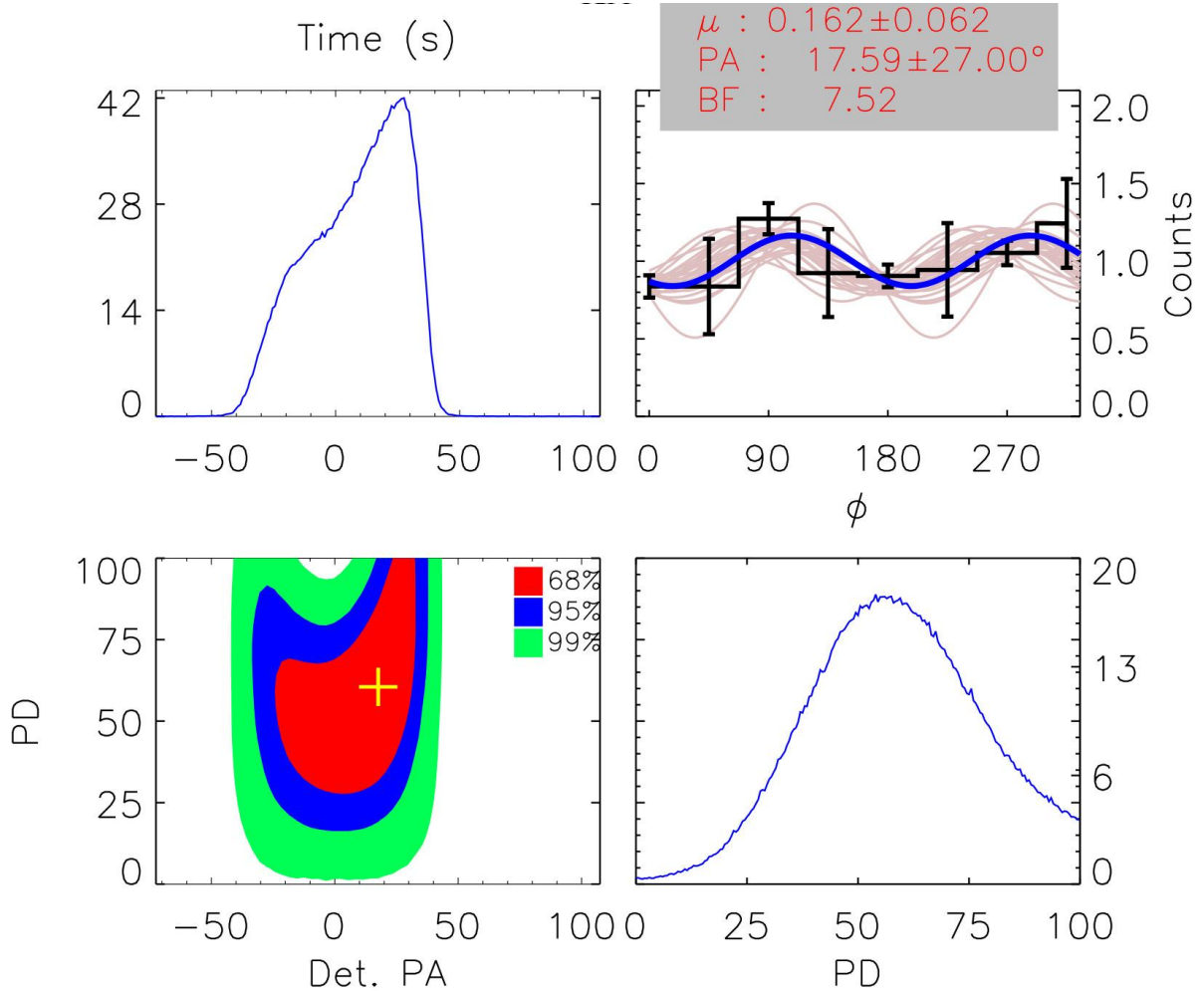

Figure 4.3: Integrated MCMC results for GRB 180427A. From MCMC iterations, top left: Posterior probability distribution for polarization angle. In the upper right corner, there are 100 random MCMC iterations along with the modulation curve and the sinusoidal fit, which are both depicted as solid blue lines. The polarization angle and degree contour map at 68%, 95%, and 99% confidence levels may be seen in the bottom left corner. Posterior probability distribution for the degree of polarization from MCMC iterations is shown in the bottom right.

4.1.2 GRB 190928A
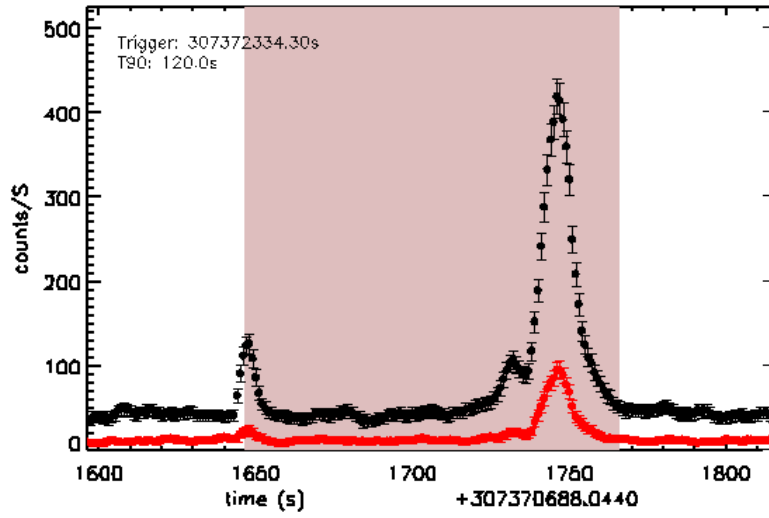
Figure 4.4: The GRB 190928A light curve. For polarization research, the light curve's shaded prompt emission phase is employed.
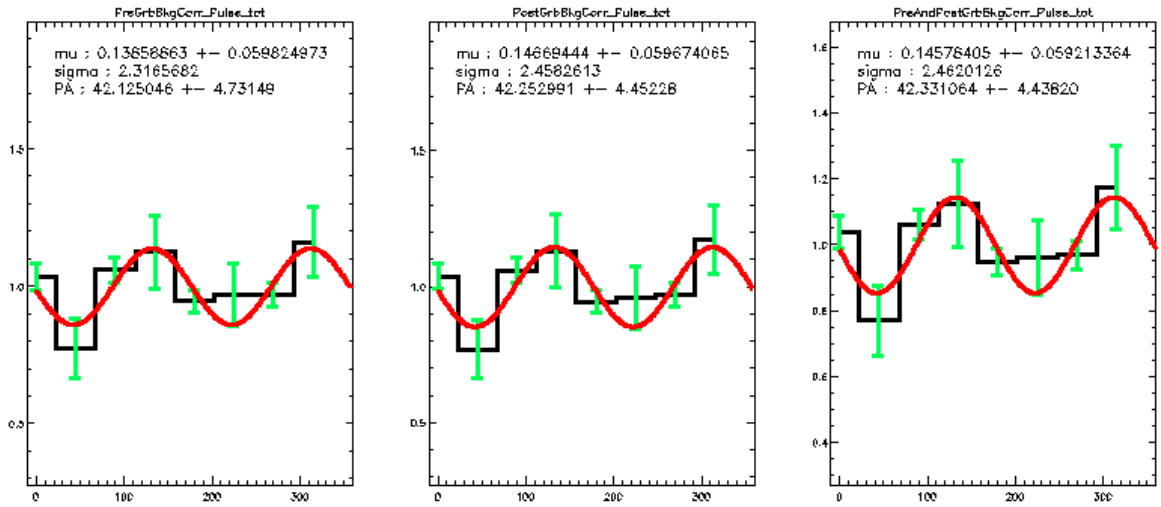
Figure 4.5: Fitted Modulation curve for GRB 190928A. The pre-GRB background radiation's adjusted modulation curve is shown on the graph to the left. The corrected modulation curve for the background radiation from post-GRB is shown in the middle of the graph. The corrected modulation curve for the background radiation before and after a GRB is shown in the graph to the right.

Figure 4.3: Integrated MCMC results for GRB 190928A. From MCMC iterations, top left: Posterior probability distribution for polarization angle. In the upper right corner, there are 100 random MCMC iterations along with the modulation curve and the sinusoidal fit, which are both depicted as solid blue lines. The polarization angle and degree contour map at 68%, 95%, and 99% confidence levels may be seen in the bottom left corner. Posterior probability distribution for the degree of polarization from MCMC iterations is shown in the bottom right.
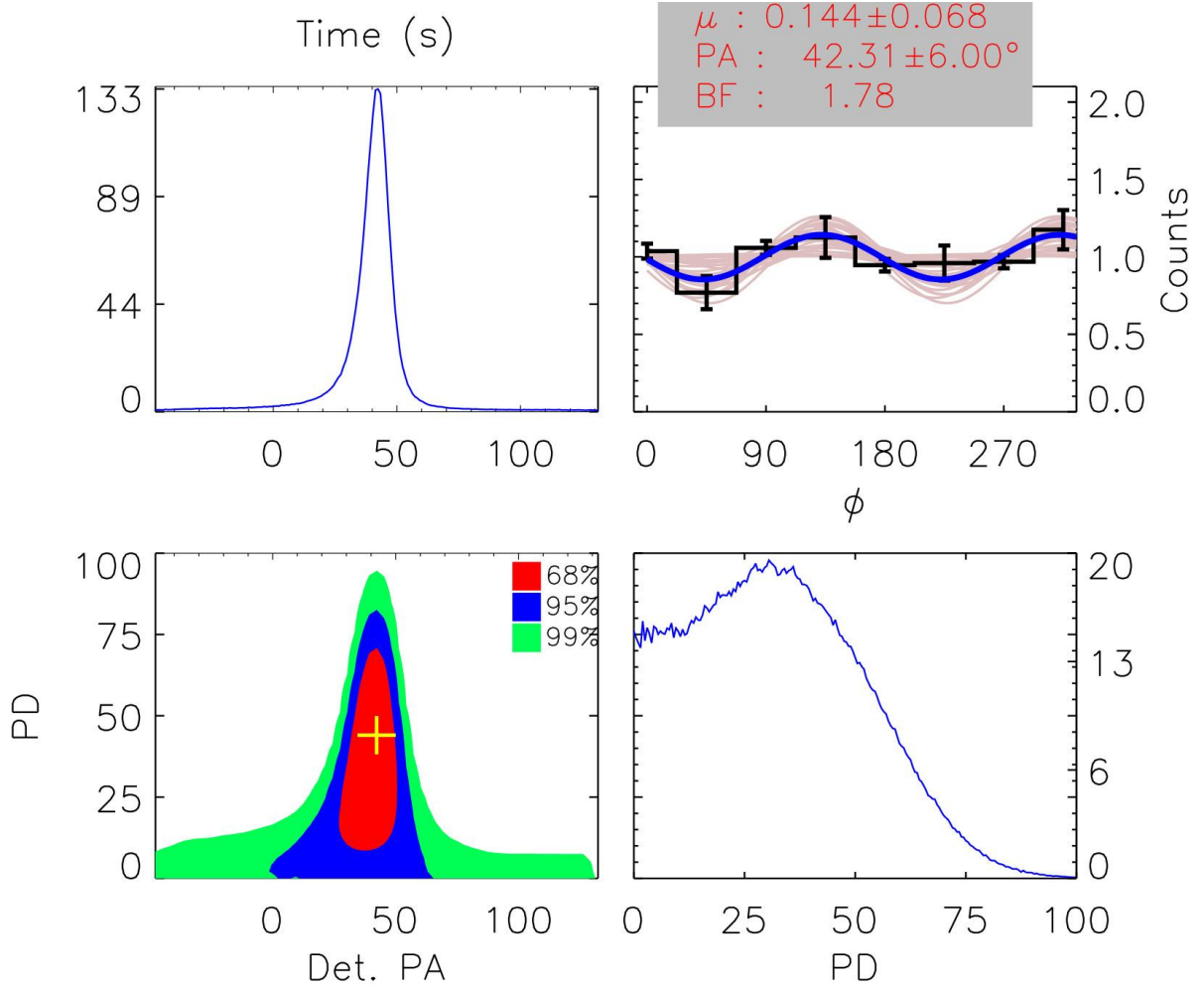
4.2 Discussions

The Compton events throughout the whole burst period with energies ranging from 100 to 600 keV are used for polarization analysis. The Compton events light curve for each GRB is displayed, emphasizing the area of prompt emission chosen for the polarization investigation (figure 4.1 and 4.4). According to equation 1 or 2, a sinusoidal function is fitted to the azimuthal angle distribution of the valid Compton events to produce a modulation curve. Each plot shows the estimated polarization angle and polarization percentage, which

are determined after accounting for the pre, post, and pre-post GRB background radiation, respectively (figure 4.2 and 4.5).

The outcomes of the MCMC simulations used to calculate the polarization angle and polarization percentage are shown on an integrated map. Figure 4.3 and Figure 4.6. The integrated plot's upper right corner shows the modulation curve after background removal and the sinusoidal fit (solid blue line). The distribution of the sinusoidal fits for 100 random iterations is also provided as solid pink lines [2]. The polarization fraction and angle contours for the two GRBs are shown in the bottom left plot of the integrated figure in the colors red, blue, and green, respectively. The top left and bottom right corners of the integrated graphic, respectively, display the posterior probability distributions for polarization angle and polarization degree. We estimate the Bayes factor to support the assertion that the burst is actually polarized (refer to section 3.4). Here, a tabular style is used to summarize and display the findings for both GRBs. Reference Table 2.

Name of the GRB	Number of Compton Events	CZTI Polarization angle (degrees)	Polarization Fraction	Bayes Factor
GRB 180427A	1153	17.59 ± 27.00	0.162 ± 0.062	7.52
GRB 190928A	5936	42.31 ± 6.00	0.144 ± 0.068	1.78

Table 2: Summarized results for GRB 180427A and GRB 190928A. The columns of the table represent the registered number of Compton events for polarization study, Polarization angle with respect to the plane of CZTI and Bayes Factor: the likelihood of polarization of source.

The criteria required to evaluate whether a source is indeed polarized and the chance of unpolarized radiation emulating such sinusoidal modulation are both minimal if the bayes factor is greater than 2, as was previously mentioned in section 3.4. It may be deduced that GRB 180427A is polarized while GRB 190928A is unpolarized because the calculated Bayes factor for GRB 180427A is 7.52 (> 2) and the Bayes factor for GRB 190928A is 1.78 (< 2).

CHAPTER 5

CONCLUSIONS AND FUTURE SCOPE

5.1 Conclusion

In the fireball model, the prompt emission is caused by highly relativistic material interacting within the jet, and the afterglow phase is caused by the jet interacting with the surrounding medium. Despite the fact that thermal emission from an expanding photosphere and inverse Compton scattering are also thought to play a significant role in many GRBs, synchrotron emission is still thought to be the primary emission mechanism for GRBs that emit rapidly [2], [3]. Examining the polarization's relationship to the spectral and temporal evolution of the GRBs could be a useful method for separating these different hypotheses. The CZTI instrument of AstroSat is used in this study to discuss the polarimetric analysis method for GRBs and to give the polarization measurements of the immediate emission for two bright GRBs. Due to the experiment's severe photon starvation [3], obtaining a trustworthy polarization measurement in hard X-rays is incredibly difficult. This characteristic is considerably amplified when measuring the polarization of a GRB's prompt emission because the prompt emission only lasts for a brief period of time. It is clear from the fact that polarization hasn't been definitively detected despite numerous tries.

The current work is extremely important in this perspective. However, given the sample space of GRBs employed in this study, it would not be reasonable to infer from the data that 50% of GRBs exhibit a large polarization percentage while the other 50% do not. (See subsection 4.2.)

5.2 Future Scope

A considerably bigger sample set is required to support the statistics in order to make definite judgments regarding whether synchrotron emission, Compton scattering, or other mechanisms are at the core of the mechanism of rapid emission. Our understanding of GRB prompt emission will be considerably improved by the availability of numerous such measurements. More of these spectropolarimetric measurements will be possible in the future thanks to specialized polarimetric devices like LEAP, POLAR-2, Daksha 2, etc [2].

BIBLIOGRAPHY

1. Tanmoy Chattopadhyay (2021). Hard X-ray polarimetry—an overview of the method, science drivers, and recent findings. *Journal of Astrophysics and Astronomy, 42(2)*.

2. Tanmoy Chattopadhyay, Soumya Gupta, Shabnam Iyyani, Divita Saraogi, Vidushi Sharma, Anastasia Tsvetkova, Ajay Ratheesh, Rahul Gupta, N. P. S. Mithun, C. S. Vaishnava, Vipul Prasad, E. Aarthy, Abhay Kumar, A. R. Rao, Santosh Vadawale, Varun Bhalerao, Dipankar Bhattacharya, Ajay Vibhute, & Dmitry Frederiks (2022). Hard X-Ray Polarization Catalog for a Five-year Sample of Gamma-Ray Bursts Using AstroSat CZT Imager. *The Astrophysical Journal, 936(1), 12*.

3. Tanmoy Chattopadhyay, Santosh V. Vadawale, E. Aarthy, N. P. S. Mithun, Vikas Chand, Ajay Ratheesh, Rupal Basak, A. R. Rao, Varun Bhalerao, Sujay Mate, Arvind B., V. Sharma, & Dipankar Bhattacharya (2019). Prompt Emission Polarimetry of Gamma-Ray Bursts with the *AstroSat* CZT Imager. *The Astrophysical Journal, 884(2), 123*.

4. Philip Kaaret. (2016). X-Ray Polarimetry.

5. Ramandeep Gill, Merlin Kole, & Jonathan Granot. (2021). GRB Polarization: A Unique Probe of GRB Physics.

6. Carolyn Kierans, Tadayuki Takahashi, & Gottfried Kanbach. (2022). Compton Telescopes for Gamma-ray Astrophysics.

7. Kolb, U. (2010). *Extreme Environment Astrophysics*. Cambridge University Press.
8. Rybicki, G., & Lightman, A. (1991). *Radiative Processes in Astrophysics*. John Wiley & Sons.

9. Vedrenne, G., & Atteia, J.L. (2009). *Gamma-Ray Bursts*. Springer.